Chemical Science

ROYAL SOCIETY OF CHEMISTRY

EDGE ARTICLE

View Article Online
View Journal | View Issue

Cite this: *Chem. Sci.*, 2022, **13**, 1030

All publication charges for this article have been paid for by the Royal Society of Chemistry

Divergent stereochemical outcomes in the insertion of donor/donor carbenes into the C–H bonds of stereogenic centers†

Sarah N. Dishman, Croix J. Laconsay, James C. Fettinger, Dean J. Tantillo and Jared T. Shaw *

Received 20th August 2021
Accepted 18th December 2021

DOI: 10.1039/d1sc04622e

rsc.li/chemical-science

Intramolecular C–H insertions with donor/donor dirhodium carbenes provide a concise and highly stereoselective method to set two contiguous stereocenters in a single step. Herein, we report the insertion of donor/donor carbenes into stereogenic carbon centers allowing access to trisubstituted benzodihydrofurans in a single step. This study illuminates, for the first time, the stereochemical impact on the carbene center and delineates the structural factors that enable control over both stereogenic centers. Sterically bulky, highly activated C–H insertion centers exhibit high substrate control yielding a single diastereomer and a single enantiomer of product regardless of the catalyst used. Less bulky, less activated C–H insertion centers exhibit catalyst control over the diastereomeric ratio (dr), where a single enantiomer of each diastereomer is observed with high selectivity. A combination of experimental studies and DFT calculations was used to elucidate the origin of these results. First, hydride transfer from the stereogenic insertion site proceeds with high stereoselectivity to the carbene center, thus determining the absolute configuration of the product. Second, the short lived zwitterionic intermediate can diaster-eoselectively ring-close by a hitherto unreported S_E2 mechanism that is either controlled by the substrate or the catalyst. These results demonstrate that donor/donor carbenes undergo uniquely stereoselective reactions that originate from a stepwise reaction mechanism, in contrast to the analogous concerted reactions of carbenes with one or more electron-withdrawing groups attached.

Introduction

The insertion of metal carbenes into C–H bonds enables the efficient and stereoselective synthesis of a wide array of complex organic molecules.[1] Most metal carbenes derive their high reactivity from having one or more electron-withdrawing groups to confer high electrophilicity. Carbenes with one electron-donating group (*e.g.* a phenyl or styrenyl) and one electron-withdrawing group are denoted as "donor/acceptor" carbenes and exhibit exquisite regio- and stereoselectivity in intermolecular insertions.[2–4] More recently, carbenes lacking any electron-withdrawing groups, *i.e.*, "donor/donor carbenes" have been employed in intra- and intermolecular reactions.[5–10] The reduced electrophilicity of donor/donor carbenes enables a high degree of functional group tolerance and the accessibility of generating the diazo carbene precursors *in situ* provides excellent scalability and safety.[11] Donor/donor carbenes often have two pendant aryl rings, where the dihedral angle between one of the aryl rings and the carbene center has been shown to affect the donor character of the ring.[12] Herein, we report C–H insertion reactions of donor/donor carbenes into stereogenic carbon centers which allow for stereoselective access to trisubstituted benzodihydrofuran cores in a single step. For the first time, this study highlights the stereochemical impact on the carbene center and provides experimental evidence supported by rigorous computations that delineates the structural factors that enable control over both stereogenic centers. This facile method to generate trisubstituted benzodihydrofuran cores enables the asymmetric synthesis of multiple classes of natural products, patented biologically active small molecules, and their analogs, to be rapidly synthesized (Fig. 1).[13–19]

Previous work by Taber[20] and Doyle[21] used chiral C–H insertion centers and acceptor-substituted carbenes to create selectivity models for their respective systems. Taber demonstrated that the stereochemistry of the C–H insertion site was retained and attributed this observation to a concerted mechanism (Fig. 2A). The stereochemical outcome of the carbene center was not evaluated due to the high enolizability of the product and its subsequent decarboxylation. Similarly, Doyle used a chiral substrate and demonstrated retention of configuration as well as catalyst-controlled regiochemistry (Fig. 2A). Again, the fate of the carbene center was not examined because

Department of Chemistry, University of California, One Shields Avenue, Davis, California 95616, USA. E-mail: jtshaw@ucdavis.edu

† Electronic supplementary information (ESI) available. CCDC 2096009, 2096010 and 2096011. For ESI and crystallographic data in CIF or other electronic format see DOI: 10.1039/d1sc04622e

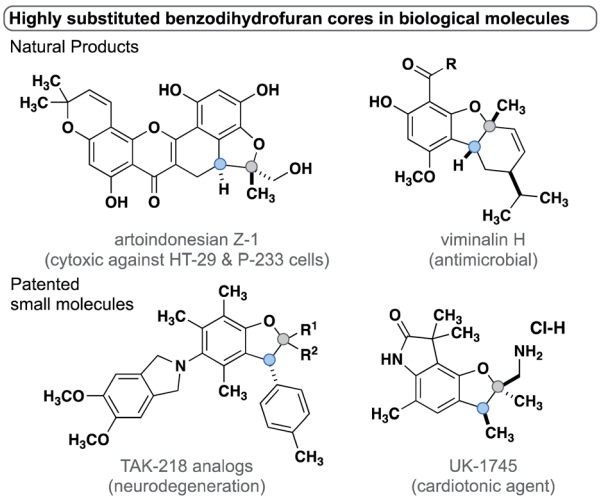

Fig. 1 Natural products and patented small molecules containing trisubstituted benzodihydrofuran cores.

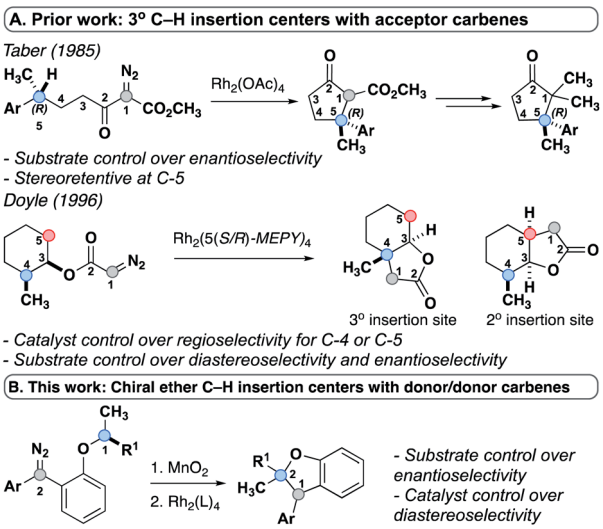

Fig. 2 (A) Prior work-tertiary C–H insertion centers with acceptor carbenes. (B) This work-donor/donor carbenes with chiral tertiary C–H insertion centers.

that carbon was non-stereogenic in the product. To date, no experimental studies have examined the stereochemical impact of insertion reactions of donor/donor carbenes. While acceptor-substituted carbenes undergo C–H insertion by a concerted mechanism, a previous study by our group hypothesized a stepwise mechanism *via* an ylide intermediate for donor/donor carbenes.[7] However, the specific factors governing stereoselectivity at each step were not explored and only an achiral catalyst was modeled. The use of chiral ether C–H insertion centers, reported within, provides for the first time experimental evidence that highlights the components governing stereoselectivity, and suggests that the formation of two new stereogenic centers may be influenced by both the substrate and the catalyst (Fig. 2B).

Results and discussion

The level of stereocontrol the substrate and catalyst impart on the C–H insertion reaction was assessed with two ether substrates and two catalysts. Ethers **1** and **2** (Fig. 3) each have a stereogenic insertion site with varying levels of reactivity based on the different stabilities of the oxocarbenium intermediate resulting from hydride transfer. Substrate **1** has a benzylic site that is highly reactive toward C–H insertion and a *p*-cyano group on the phenyl donor core to enable subsequent derivatization for crystallography and separation by chiral HPLC (see ESI Fig. 2†). Notably, previous work by our group shows that electronic variation of the phenyl donor core doesn't affect the enantiomeric ratio (er) significantly.[7] The chiral homoallylic ether, substrate **2**, is less activated toward C–H insertion because there is no stabilization of the cation intermediate *via* resonance. The homoallylic ether also enabled better separation by chiral HPLC and the opportunity to obtain a crystalline derivative (see ESI Fig. 2†). Each C–H insertion reaction could potentially yield two diastereomers and their respective enantiomers. Both racemic and enantiopure substrates were used with chiral dirhodium catalysts (*R*-**3** and *S*-**3**) as well as the achiral catalyst $Rh_2(mes\text{-}CO_2)_4$ (**4**) (Fig. 3). The experimental data collected from multiple substrate and catalyst pairings enabled stereochemical trends to be identified and studied further using DFT calculations (*vide infra*).

Initial studies involved substrate **1**, containing a highly activated and bulky C–H insertion center substituted with methyl and phenyl groups. Both racemic **1** and enantiopure **1** yielded the benzodihydrofuran product as a single cis diastereomer (**5a**, Table 1, entries 1–3) irrespective of which catalyst was used. The enantioselectivity followed a similar trend where racemic **1** provided racemic **5a** and enantiopure **1** gave a single enantiomer of **5a** in 97 : 03 er (Table 1, entries 4–6) regardless of the catalyst employed in the reaction. Therefore, these substrates with highly activated sterically occluded C–H insertion centers elicit highly stereoselective substrate-controlled C–H insertion reactions.

The diastereoselectivity of the reaction with **1** is not influenced by the structure of the catalyst whereas the enantioselectivity is dictated by the configuration at the carbon undergoing insertion. These results are consistent with those of Taber and Doyle in that the configuration of the insertion site of (*S*)-**1** is retained in product **5a**, *i.e.*, consistent with a concerted C–H insertion mechanism. The differential results from (*R*/*S*)-**1**

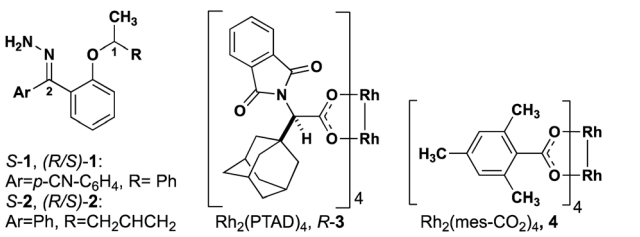

Fig. 3 Structures of hydrazone precursors and commonly used dirhodium catalysts with donor/donor carbene C–H insertion systems.

Table 1 Alkyl/aryl stereogenic insertion centers

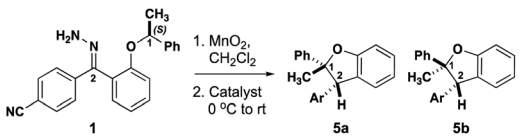

Entry	SM	Catalyst	dr[a] **5a** : **5b**	er[b] (**5a**) (*R*,*S*) : (*S*,*R*)	Yield (%)
1	(*R*/*S*)-**1**	*R*-**3**	>95 : 5	49 : 51	68
2	(*R*/*S*)-**1**	*S*-**3**	>95 : 5	49 : 51	65
3	(*R*/*S*)-**1**	4	>95 : 5	49 : 51	65
4[c]	(*S*)-**1**	*R*-**3**	>95 : 5	97 : 03	82
5	(*S*)-**1**	*S*-**3**	>95 : 5	97 : 03	71
6	(*S*)-**1**	4	>95 : 5	97 : 03	76

[a] dr determined by ^{1}H NMR analysis of unpurified reaction mixtures. [b] er determined by chiral HPLC. [c] Absolute stereochemistry confirmed by X-ray crystallography.

and (*S*)-**1** suggest that the configuration at the insertion site (C-1) dictates the configuration at C-2 during the insertion reaction. These data do not rule out a highly stereoselective stepwise mechanism.

Based on the results above, a less activated, less bulky C–H insertion center substituted with methyl and homoallylic groups (**2**) was examined to see if diastereo- or enantiocontrol over the reaction differed from **1** (Table 2). Interestingly, the C–H insertions reactions of these less activated substrates showed drastically different stereoselectivity trends compared to the alkyl/aryl substrates. Racemic **2** yielded a 47 : 53 and 48 : 52 dr of **6a** : **6b** with *R*-**3** and *S*-**3** respectively (Table 2, entries 1–2). There was a slight enrichment towards the trans diastereomer (**6a**) with **4** yielding a 57 : 43 dr (Table 2, entry 3). Strikingly, when the er was measured the chiral catalysts generated each diastereomer of **6** in high er (Table 2, entries 1–2), while the achiral catalyst yielded racemic mixtures of each diastereomer of **6**. While substrate (*R*/*S*)-**1** led only to racemic products, (*R*/*S*)-**2** can be steered toward enantio-enriched products with the chiral catalysts.

The results with (*S*)-**2** were even more striking. Treatment of this substrate with *R*-**3** resulted in preferential formation of trans benzodihydrofuran **6a** (Table 2, entry 4) with high enantioselectivity. Use of the same substrate with *S*-**3** resulted in inverted diastereoselectivity with the same enantiomeric preference as the reaction with *R*-**3** (Table 2, entry 5)! The eroded enantioselectivity for the formation of **6a** in this case highlights the mismatch in stereochemical preference between the substrate and the catalyst. Finally, the insertion of (*S*)-**2** with achiral catalyst (**4**) showed little diastereoselectivity while retaining the high substrate-induced enantioselectivity (Table 2, entry 6). On one hand, these results demonstrate that the stereogenic center undergoing insertion controls the magnitude and orientation of enantioselectivity for both newly formed stereogenic centers in the product. The catalyst, on the other hand, can have a strong influence on the diastereoselectivity, and (*R*/*S*)-**3** is a privileged catalyst scaffold for this system.[7] These results are consistent with a highly stereoselective hydride transfer step that is followed by a diastereoselective ring closure that can be controlled by the configuration of the catalyst.

To investigate the C–H insertion mechanism leading to **6** and delve further into the origins of the observed stereocontrol, we turned our attention to computational studies. Density functional theory (DFT) calculations have previously aided our study of C–H insertion mechanisms of donor/donor carbenes.[7] However, unlike previous DFT explorations of similar reactions in which the Rh catalyst can be reasonably modeled with $Rh_2(OAc)_4$, or even $Rh_2(HCO_2)_4$,[22] we could only adequately investigate the current mechanistic question by modeling the insertion reaction of **6** within the chiral cavity[23,24] of either Rh_2(*R*-PTAD)$_4$ or Rh_2(*S*-PTAD)$_4$. Given the size of the *N*-phthalimido and adamantyl ligands on Rh_2(*R*-PTAD)$_4$ (weighing in at 219 atoms and 940 electrons), and the concomitant computational cost, we reasoned that truncating the adamantyl groups to methyl groups struck a sensible balance between mechanistic

Table 2 Alkyl/alkyl stereogenic insertion centers

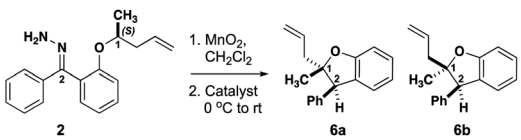

Entry	SM	Catalyst	dr[a] **6a** : **6b**	er[b]-**6a** (*S*,*R*) : (*R*,*S*)	er[b]-**6b** (*R*,*R*) : (*S*,*S*)	Yield (%)
1	(*R*/*S*)-**2**	*R*-**3**	47 : 53	91 : 09	86 : 14	70
2	(*R*/*S*)-**2**	*S*-**3**	48 : 52	11 : 89	16 : 84	68
3	(*R*/*S*)-**2**	4	57 : 43	49 : 51	50 : 50	91
4[c]	(*S*)-**2**	*R*-**3**	86 : 14	99 : 01	99 : 01	77
5	(*S*)-**2**	*S*-**3**	10 : 90	74 : 26	99 : 01	75
6	(*S*)-**2**	4	53 : 47	98 : 02	99 : 01	58

[a] dr determined by ^{1}H NMR analysis of unpurified reaction mixtures. [b] er determined by chiral HPLC. [c] Absolute stereochemistry confirmed by X-ray crystallography.

insight and cost with the modeling capabilities at our disposal.[23,24]

A stepwise mechanism involving a short lived zwitterionic intermediate was found for the reactions of substrate **2**, similar to that previously proposed for C–H insertions of donor/donor carbenes with primary, achiral insertion sites[7] (see computational ESI† for details; all computed structures can be found in the ioChem-BD repository[25]). For clarity, the mechanism for formation of one enantiomer of the major diastereomer from diazo compound **7** is shown in Fig. 4 (see ESI Fig. 4–5† for detailed reaction profiles for formation of the other diastereomer and its enantiomer). First, addition of the chiral catalyst results in a tetrahedral intermediate (**11**) with N_2 poised to leave. The free energy barrier to extrude nitrogen is low (overall, a 6.2 kcal mol^{-1} barrier from **7**) and this process is predicted to be highly exergonic ($\Delta G = -32.2$ kcal mol^{-1}), forming one major rotamer of Rh carbene (**8**). From **8**, an initial hydride-shift from C-1 to C-2 is followed by an S_E2 C–C bond closure step to yield the major product (**6a**).[26] The hydride transfer occurs with high stereochemical fidelity, accounting for the high selectivity of the newly formed stereogenic center at C-2. The diastereomeric ratio observed is hypothesized to be due to the major oxocarbenium ion intermediate (**9**) rotating about the C_{aryl}–O bond, preferentially exposing one prochiral face based on the configuration of the catalyst. Although our computed mechanism is formally stepwise, the C–H insertion event can be considered to border the realm of a concerted, highly asynchronous mechanism (see ESI Fig. 3†).[27]

Although we successfully identified transition states leading from **9** to **6a** and from **10** to **6b** (ESI Fig. 4–5†), the transition state for conversion of **9** to **10** remains elusive. The observed 85 : 15 ratio results from the relative energy of these two transition states, as well as the interconversion of **9** to **10**. While it is difficult to disentangle the exact influence of these three transition states on diastereoselectivity, the data are consistent with an oxocarbenium ion whose stereochemical fate is determined

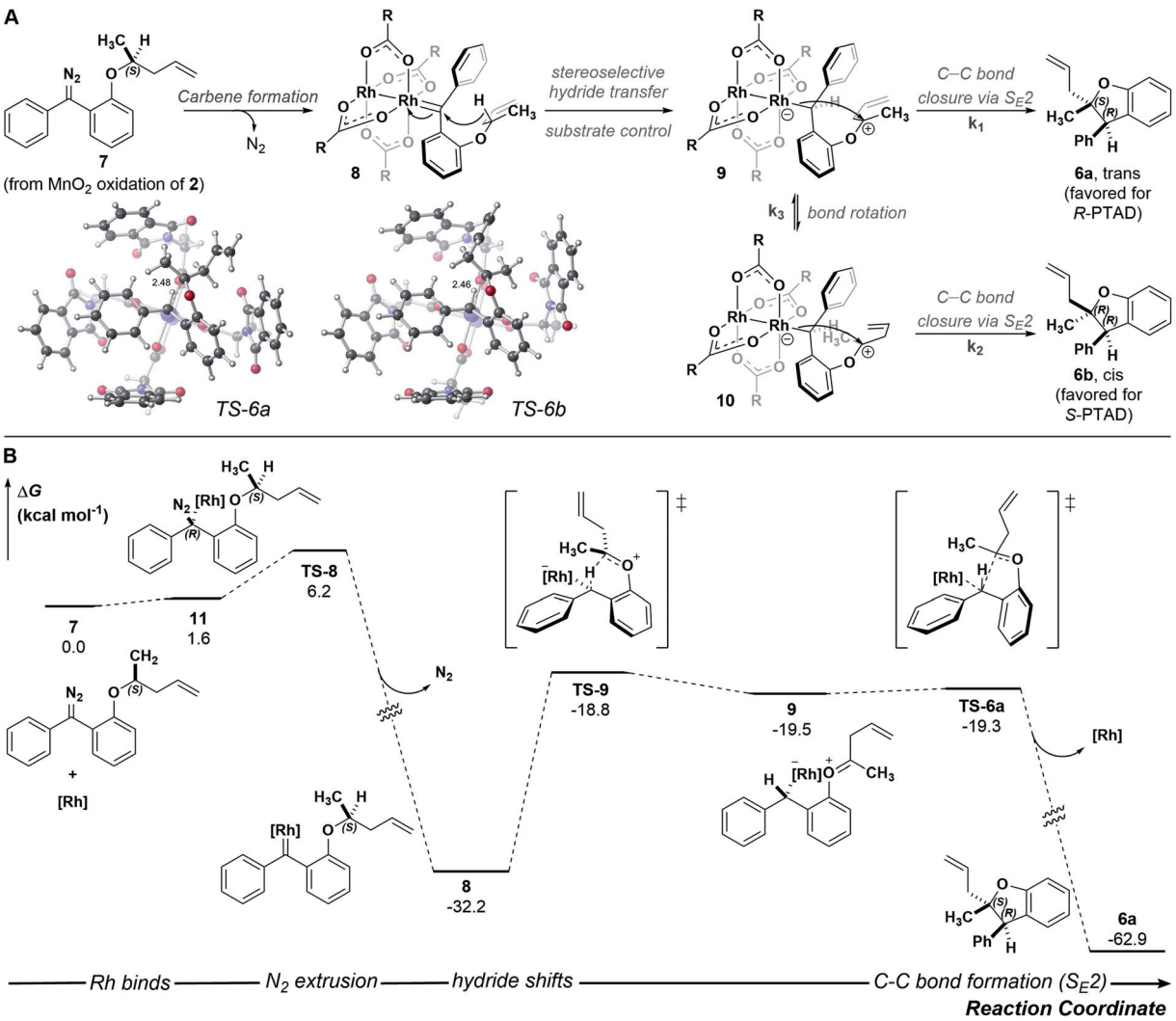

Fig. 4 (A) Arrow-pushing mechanism and S_E2 transition-state structures leading to **6a** and **6b** (see ESI† for **TS-6b**). (B) Reaction energy profile computed with DFT at the PCM(CH_2Cl_2)-B3LYP-D3(BJ)/SDD[6-31+G(d,p)]//PCM(CH_2Cl_2)-B3LYP-D3(BJ)/LANL2DZ[6-31G(d)] level of theory; [Rh] = Rh_2(*R*-PTAD)$_4$.

by the catalyst. Small perturbations resulting from factors not explicitly modeled here, *e.g.*, explicit solvent effects, deviations in the chiral crown structure, or non-statistical dynamic effects, could account for issues in delineating these three steps' effects on the diastereoselectivity.[28–33] Results in the ESI Fig. 4 and 5† corroborate the experimental enantioselectivity: specifically formation of pro-chiral *R*-**3** bound Rh-carbene intermediate (SI-23) leading to (*R*,*S*)-**6a** is kinetically and thermodynamically unfavorable ($\Delta\Delta G‡ = 4.3$ kcal mol^{-1} and $\Delta\Delta G = 3.9$ kcal mol^{-1} relative to 7) compared to that leading to (*S*,*R*)-**6a**, consistent with an er of 99 : 1 at 0 °C (Table 2, entry 4).

This stepwise pathway can be used to hypothesize a similar mechanism for **5a** (Fig. 5). Oxidation of (*S*)-**1** to diazo followed by addition of catalyst will form Rh carbene **12**. This intermediate will undergo the same highly stereoselective hydride transfer to form a single **13**. Rotating about the C_{aryl}–O bond in **13** to expose the other prochiral oxocarbenium ion face is likely kinetically unfavorable due to increased steric bulk of the phenyl ring, contributing to a high energic cost to rotate in the chiral cavity. Our computational results from an energy surface scan with an achiral catalyst indicate that rotation about the C_{aryl}–O bond in **13** indeed requires more energy (>4 kcal mol^{-1}) than C–C bond formation (ESI Fig. 9†). Therefore, **13** rapidly closes to form a new C–C bond by an S_E2 mechanism yielding **5a** as the single enantiomer and single diastereomer of product. The computed pathway for the carbene intermediate of substrate **1** reacting with $Rh_2(OAc)_4$ supports a stepwise mechanism for the C–H insertion event: the intermediacy of an oxocarbenium ion results from hydride transfer that proceeds to **5a** through an S_E2 mechanism, similar to what is observed for **9** proceeding to **6a**. This mechanistic model enables rapid assessment of new substrates. If a racemic substrate results in low diastereoselectivity with an achiral catalyst, as was the case with **2**, we predict that it is possible to observe high diastereoselectivity with a single enantiomer of starting material and a chiral catalyst. If, on the other hand, a substrate exhibits high diastereoselectivity under the same circumstances, we predict it will probably be impossible to favor the minor diastereomer under any circumstances.

In all cases, high enantioselectivity for both diastereomers can be expected to result from an enantiomerically pure substrate regardless of catalyst chirality. Seven additional substrates are illustrative of these generalizations (Fig. 6).

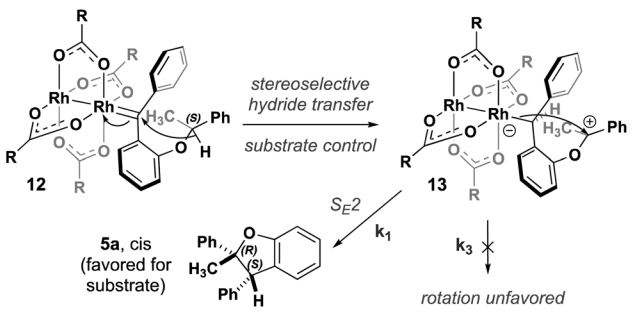

Fig. 5 Proposed arrow pushing mechanism leading to **5a**.

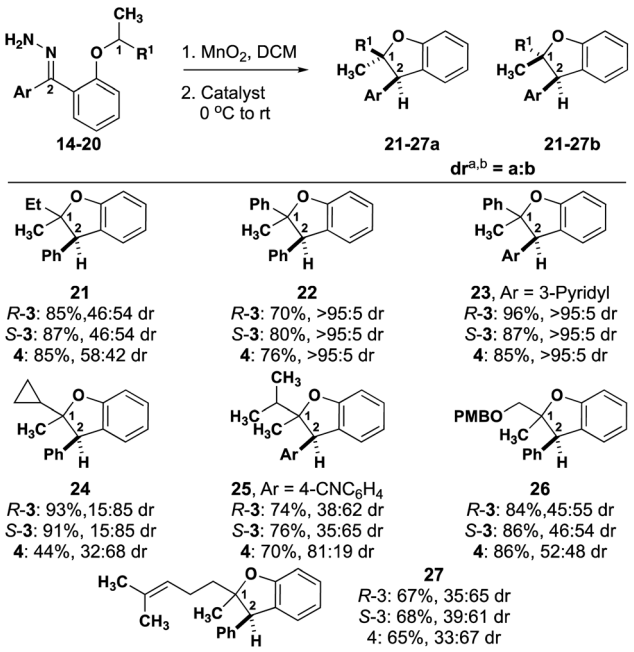

Fig. 6 Substrate scope for varying electronic activation and steric bulk at the C–H insertion center. [a] dr determined by ^{1}H NMR analysis of unpurified reaction mixtures. [b] Assigned diastereomers determined from analogous compound NMR shifts.

An *n*-alkyl substrate (**21**, R = Et) behaves much like **2**, exhibiting little substrate control, offering the opportunity for catalyst control. Similarly, substrate **26**, enables catalyst control over the dr. Substrate **22**, which is analogous to **1**, exhibits high substrate control, and substitution of the phenyl rings with a heterocycle, substrate **23**, doesn't affect selectivity. A shorter branched alkyl substrate (**25**, R = *i*-Pr) is intermediary, with a substrate preference that is opposite to what is preferred by either enantiomer of catalyst **3**. A longer branched alkyl substrates (**27**, R = prenyl) is analogous to **25**, where there is slight substrate preference for one diastereomer. Finally, **24** (R = *c*Pr) exhibits a slight preference for one diastereomer with catalyst **4** that is enhanced by either enantiomer of catalyst. It is possible in the cases of **22** and **23** that a particular substrate/catalyst pairing will enable high diastereoselectivity, but the inherent substrate control exhibited by the achiral catalyst suggests that favoring the other diastereomer will be more challenging than it is for **2** and **21**.

Conclusions

In summary, we have developed a method and stereochemical rationale for intramolecular C–H insertion reactions with donor/donor carbene systems having chiral ethers. This enables the generation of two contiguous stereogenic centers in a single step, yielding a trisubstituted benzodihydrofuran core. Exploration of chiral substrates with two enantiomers of a chiral catalyst revealed stereoselectivity patterns not observed with other types of carbene C–H insertion systems. High enantioselectivity can be achieved and controlled based on the

enantiomer of starting material used. For sterically occluded and highly activated C–H insertion centers, high diastereoselectivity emerges from substrate control, irrespective of the catalyst used. Less sterically demanding and less activated C–H insertion centers exhibit high diastereoselectivity that is controlled based on the enantiomer of catalyst employed in the reaction. Our DFT studies with a truncated variant of the chiral Rh_2(*R*-PTAD)$_4$ catalyst demonstrate that the highly stereoselective hydride transfer controls enantioselectivity outcomes, whereas a zwitterionic intermediate undergoes diastereoselective ring closure through an S_E2 mechanism. These studies demonstrate that donor/donor carbenes are capable of unique levels of stereocontrol not previously seen with carbenes appended with one or more electron-withdrawing group.‡

Data availability

All optimized structure coordinates are reported on the ioChem-BD database. These structures can be found at the following DOI: https://doi.org/10.19061/iochem-bd-6-94. Crystallographic data for compounds **43–45** have been deposited at the CCDC under 2096009, 2096010, and 2096011.

Author contributions

The manuscript was written through contributions from all authors. All authors have given approval to the final version of the manuscript.

Conflicts of interest

There are no conflicts to declare.

Acknowledgements

This work was supported by grants from the National Institutes of Health (R01/GM124234) and National Science Foundation (CHE-1856416 and XSEDE). We thank the Franz group (UC Davis) for providing access to a chiral HPLC and particularly Jake Jagannathan (Franz Group, UC Davis) for providing assistance with HPLC traces. We also thank the Kurth group (UC Davis) for use of their IR with assistance from the Olson Group (UC Davis). We thank the National Science Foundation (Grant CHE-1531193) for the Dual Source X-ray diffractometer.

Notes and references

‡ This work was previously posted as a preprint on ChemRxiv.[34]

1 D. J. Abrams, P. A. Provencher and E. J. Sorensen, *Chem. Soc. Rev.*, 2018, **47**, 8925–8967.
2 M. P. Doyle, R. Duffy, M. Ratnikov and L. Zhou, *Chem. Rev.*, 2010, **110**, 704–724.
3 J. Fu, Z. Ren, J. Bacsa, D. G. Musaev and H. M. L. Davies, *Nature*, 2018, **564**, 395–399.
4 H. M. L. Davies and K. Liao, *Nat. Rev. Chem.*, 2019, **3**, 347–360.
5 J. R. Jagannathan, J. C. Fettinger, J. T. Shaw and A. K. Franz, *J. Am. Chem. Soc.*, 2020, **142**, 11674–11679.
6 W. H. Cheung, S. L. Zheng, W. Y. Yu, G. C. Zhou and C. M. Che, *Org. Lett.*, 2003, **5**, 2535–2538.
7 K. N. Lamb, R. A. Squitieri, S. R. Chintala, A. J. Kwong, E. I. Balmond, C. Soldi, O. Dmitrenko, M. Castiñeira Reis, R. Chung, J. B. Addison, J. C. Fettinger, J. E. Hein, D. J. Tantillo, J. M. Fox and J. T. Shaw, *Chem.–Eur. J.*, 2017, **23**, 11843–11855.
8 B. D. Bergstrom, L. A. Nickerson, J. T. Shaw and L. W. Souza, *Angew. Chem., Int. Ed.*, 2021, **60**, 6864–6878.
9 C. Soldi, K. N. Lamb, R. A. Squitieri, M. González-López, M. J. Di Maso and J. T. Shaw, *J. Am. Chem. Soc.*, 2014, **136**, 15142–15145.
10 D. Zhu, L. Chen, H. Fan, Q. Yao and S. Zhu, *Chem. Soc. Rev.*, 2020, **49**, 908–950.
11 J. Ma, L. Zhang and S. Zhu, *Curr. Org. Chem.*, 2016, **20**, 102–118.
12 M. Lee, Z. Ren, G. Musaev and H. M. L. Davies, *ACS Catal.*, 2020, **10**, 6240–6247.
13 I. Musthapa, J. Latip, H. Takayama, L. D. Juliawaty, E. H. Hakim and Y. M. Syah, *Nat. Prod. Commun.*, 2009, **4**, 927–930.
14 T. Suhartati, S. A. Achmad, N. Aimi, E. H. Hakim, M. Kitajima, H. Takayama and K. Takeya, *Fitoterapia*, 2001, **72**, 912–918.
15 J. Q. Cao, H. Y. Tian, M. M. Li, W. Zhang, Y. Wang, L. Wang and W. C. Ye, *J. Nat. Prod.*, 2018, **81**, 57–62.
16 L. Wu, Y. L. Zhang, X. B. Wang, Y. M. Zhang, M. H. Yang, J. Luo and L. Y. Kong, *Tetrahedron*, 2017, **73**, 1105–1113.
17 K. Yoshinori, K. Katsumi, T. Tsutomu, O. Tadaaki, Y. Takashi, O. Kazuhiro, S. Seiichi, S. Noboru, S. Hiromichi, O. Tomio, O. Toshiaki, O. Yukihiro, S. Kimiyuki, T. Yoshio, F. Mikio and U. Yasumi, European Patent, 0653426A1, 1995.
18 H. Uemura, N. Sakamoto and H. Nakaya, *Eur. J. Pharmacol.*, 1999, **383**, 361–371.
19 O. Shigenori, A. Yasuyoshi, K. Kouki, O. Masahiro and S. Makaki, Japan Patent, 19980345355, 1998.
20 D. F. Taber and E. H. Petty, *J. Am. Chem. Soc.*, 1985, **107**, 196–199.
21 M. P. Doyle, A. V. Kalinin and D. G. Ene, *J. Am. Chem. Soc.*, 1996, **118**, 8837–8846.
22 E. Nakamura, N. Yoshikai and M. Yamanaka, *J. Am. Chem. Soc.*, 2002, **124**, 7181–7192.
23 S. Singha, M. Buchsteiner, G. Bistoni, R. Goddard and A. Furstner, *J. Am. Chem. Soc.*, 2021, **143**, 5666–5673.
24 L. Kong, X. Han, H. Chen, H. Sun, Y. Lan and X. Li, *ACS Catal.*, 2021, **11**, 4929–4935.
25 M. Álvarez-Moreno, C. de Graaf, N. Lopez, F. Maseras, J. M. Poblet and C. Bo, *J. Chem. Inf. Model.*, 2015, **55**, 95–103.
26 J. M. Fukuto and F. R. Jensen, *Acc. Chem. Res.*, 1983, **16**, 177–184.
27 D. J. Tantillo, *J. Phys. Org. Chem.*, 2008, **21**, 561–570.
28 J. Wang, B. Chen and J. Bao, *J. Org. Chem.*, 1998, **63**, 1853–1862.

29 R. S. Drago, S. P. Tanner, R. M. Richman and J. R. Long, *J. Am. Chem. Soc.*, 1979, **101**, 2897–2903.
30 A. F. Trindade, J. A. S. Coelho, C. A. M. Afonso, L. F. Veiros and P. M. Gois, *ACS Catal.*, 2012, **2**, 370–383.
31 F. Adly, *Catalysts*, 2017, **7**, 347.
32 B. K. Carpenter, *Chem. Rev.*, 2013, **113**, 7265–7286.
33 R. E. Plata and D. A. Singleton, *J. Am. Chem. Soc.*, 2015, **137**, 3811–3826.
34 S. N. Dishman, C. J. Laconsay, J. C. Fettinger, D. J. Tantillo and J. T. Shaw, *ChemRxiv*, 2021, DOI: 10.33774/chemrxiv-2021-h06nc-v2.